PHOTONICS Research

Two-photon interference between continuous-wave coherent photons temporally separated by a day

DANBI KIM, JIHO PARK, TAEK JEONG, HEONOH KIM, AND HAN SEB MOON*

Department of Physics, Pusan National University, Geumjeong-Gu, Busan 46241, South Korea
*Corresponding author: hsmoon@pusan.ac.kr

Received 4 September 2019; revised 24 December 2019; accepted 2 January 2020; posted 3 January 2020 (Doc. ID 376993); published 27 February 2020

An understanding of the phenomenon of light interference forms the kernel underlying the discovery of the nature of light from the viewpoints of both classical physics and quantum physics. Here we report on two-photon interference with temporally separated continuous-wave coherent photons by using a temporal post-selection method with an arbitrary time delay. Although the temporal separation of a day between the photons is considerably longer than the coherence time of the light source, we observe the Hong–Ou–Mandel (HOM) interference of the pairwise two-photon state. Furthermore, we experimentally demonstrate the HOM interference observed in one of the interferometer-output modes by using only one single-photon detector for a large temporal separation.

https://doi.org/10.1364/PRJ.376993

1. INTRODUCTION

The interference phenomenon forms the most important evidence of the wave-like property of light. The phase of the wave is the key concept underlying the interpretation of constructive and destructive interferences of superposed light beams. On the other hand, it is known that even when light is considered as a particle or photon, a single photon can interfere with itself [1]. Although light exhibits both wave- and particle-like properties, the linear superposition of the field amplitudes for light waves is the same as that of the probability amplitudes of a photon in the case of first-order interference.

However, beyond the classical physics perspective, we can consider quantum interference, which refers to multi-photon interference due to the quantum nature of light. The simplest multi-photon interference is two-photon interference (TPI), which is a second-order interference phenomenon; in this context, the Hong–Ou–Mandel (HOM) interference effect is a well-known two-photon quantum interference phenomenon [2]. To date, TPI has formed the basis of several quantum optics studies and optical quantum information processing applications [3–7].

In experimental quantum optics, the two-photon quantum interference of correlated photons is regarded as important evidence of the quantum nature of light fields. In this regard, many TPI experiments have been widely demonstrated with the use of quantum light sources such as photon pairs from nonlinear crystals [8], atomic ensembles [9,10], optical fibers [11], and nanophotonics devices [12]. With the use of coherent or thermal light sources, HOM-type interference has been experimentally demonstrated with a limited visibility of 0.5 [13–17]. Several intensive studies on HOM interference with classical light signals have been conducted for application to quantum information science [13–21] because it is easy to "mimic" quantum interference with this approach.

In general, the spectral, spatial, and polarization modes of the photons at the output beam splitter in an interferometry setup should be indistinguishable and superposed to realize high-visibility interference. In the case of TPI, it is intuitive to consider the temporal overlap between two photons at the beam splitter. However, although the photons arrive at the beam splitter at different times, it is possible to observe the TPI effect [22]. This interesting TPI phenomenon has been experimentally demonstrated with the use of temporally separated pulsed-mode photons [23–26].

Meanwhile, we note that the electrical or optical delay for the temporal post-selection was limited by the constraints of the delay module or the optical fiber loss. So far, the temporal separation between photons has been less than 1 s [22–26]. In this study, we experimentally demonstrate HOM interference with long temporally separated continuous-wave (CW)-mode photons by using a novel method for temporal post-selection. We investigate the visibility of HOM interference with photons temporally separated by days by applying an electrical time delay between two single-photon detectors (SPDs) for coincidence measurement. Furthermore, we measure an HOM-type fringe with CW-mode coherent light by using only a single SPD via the temporal post-selection method with an electrical delay.

2. SCHEMATIC OF COINCIDENCE MEASUREMENT

Figure 1(a) shows the schematic of the setup utilized for the coincidence measurement of two temporally separated CW-mode photons via temporal post-selection. We note that the important difference between the CW mode and pulsed mode of lasers is the localization of photons in space or time. In the case of CW coherent light, the probability amplitude of the photon continuously spreads over time in coherent light beams. Here we consider the two-photon state in paths 1 and 2, which only contribute to HOM interference through the coincidence measurement with two SPDs (D1 and D2). In the case of the CW-mode photons, the input state can be described as a superposition of all possible two-photon product states $\sum_{i=0}^{\infty} a^{\dagger} a^{\dagger}(\Delta t_i)|0,0\rangle$, where $a^{\dagger}$ represents the photon creation operator and Δt_i the separation time between sequential photons. The two photons incident on the polarizing beam splitter (PBS1) are diagonally polarized with respect to the axis of the PBS, and they can be described using the terms $a^{\dagger} = 1/\sqrt{2}(a_H^{\dagger} + a_V^{\dagger})$ and $a^{\dagger}(\Delta t_i) = 1/\sqrt{2}[a_H^{\dagger}(\Delta t_i) + a_V^{\dagger}(\Delta t_i)]$. When we consider the time-delayed coincidence counts of the two detectors, the two photons in the interferometer arms can be treated as temporally separated pairwise two-photon (TSPT) states [connected by the dashed lines in Fig. 1(a)]. In this case, the separation time can be considerably longer than the coherence time of the CW coherent light. Therefore, the two photons do not temporally cross at the output beam splitter of the interferometer. The TSPT state with Δt is described as

$$|\Psi\rangle_{\mathrm{TSPT}} = \frac{1}{\sqrt{2}}[a_1^{\dagger} a_2^{\dagger}(\Delta t_i) + a_2^{\dagger} a_1^{\dagger}(\Delta t_i)]|0,0\rangle, \quad \textbf{(1)}$$

where $a_i^{\dagger}$ denotes the photon creation operator and the subscripts represent the two spatial modes of the interferometer arms according to the two output ports of PBS1.

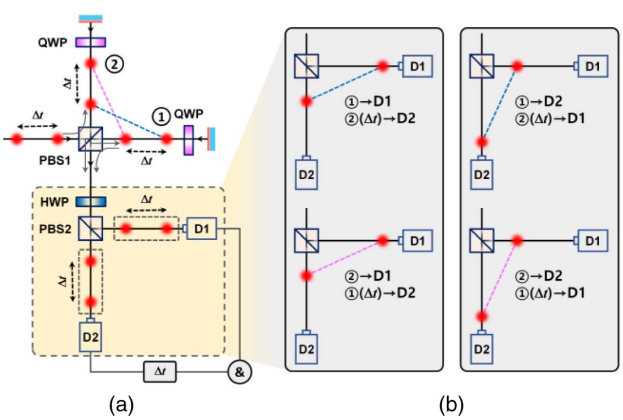

Fig. 1. (a) Schematic depicting coincidence measurement of two temporally separated CW-mode coherent photons via temporal post-selection. (b) Feynman diagrams depicting indistinguishable events of the TSPT states at the output stage.

When two photons in a TSPT state are recombined at PBS1, the two photons are probabilistically bunched in one of the two spatial modes of the two PBS2 output ports, similar to the conventional HOM interference effect. Figure 1(b) illustrates the Feynman diagrams for the two indistinguishable coincidence events of the TSPT states at the PBS2 output ports. Although the two photons are temporally well separated, the two-photon amplitudes of the TSPT states are indistinguishable in coincidence detection as shown in Fig. 1(b). The two cases presented in Fig. 1(b) correspond to the destructive interference of the two-photon probability amplitudes. Consequently, the two photons of the TSPT state are acquired at one of the two PBS2 output ports with a probability of 1/2. In the case of CW-mode photons, the temporal information of the photon is not defined; however, the relative time delay from the measured time of a photon at D1 to the coincidence measurement at D2 is well defined. In the experiment, we measured the HOM interference with the TSPT state with arbitrary values of Δt via temporal post-selection.

3. EXPERIMENTAL SETUP FOR TWO-PHOTON INTERFERENCE

Figure 2 shows the experimental schematic for HOM interference with the use of a weak CW laser via temporal post-selection utilizing a polarization-based Michelson interferometer including one mirror (M1) with a piezoelectric transducer (PZT) actuator and a second mirror (M2) with a motorized translation stage. With this setup, we measured the interference fringe as a function of the path-length difference Δx. In our experiment, we used a multi-mode diode laser with a center wavelength of 810 nm and spectral width of 2.6 nm. The collimated laser was highly attenuated to the single-photon count rate of approximately 350 kHz at the two SPDs after photon passage through an attenuator, an interference filter (IF) with 2 nm bandwidth, and PBS1 for applying linear polarization. Next, the coherent photons were equally divided along the two paths by PBS2 after passage through a half-wave plate

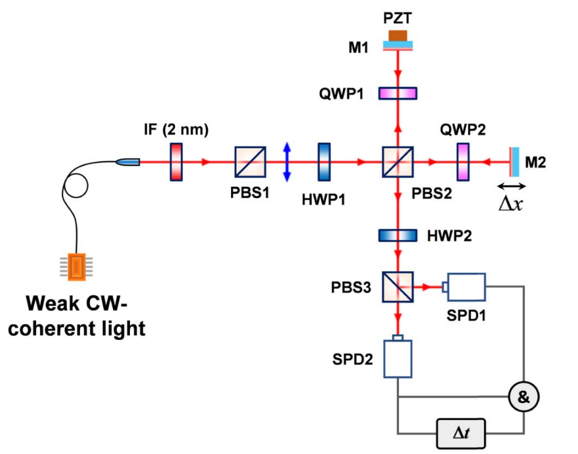

Fig. 2. Schematic of experimental setup for HOM interference with a weak CW laser via temporal post-selection with the use of a polarization-based Michelson interferometer (M, mirror; PBS, polarizing beam splitter; IF, interference filter; HWP, half-wave plate; QWP, quarter-wave plate; SPD, single-photon detector).

(HWP1) whose axis was oriented at 22.5°. Two quarter-wave plates (QWPs) with their axes oriented at 45° were also positioned along the two interferometer arms to rotate the polarization direction. The two photons from the PBS2 output port passed through HWP2 (with its axis oriented at 22.5°) and PBS3 to erase the polarization information. To measure the time-delayed coincidence counts of D1 and D2, we applied an electrical delay (Δt) at D2.

4. HOM INTERFERENCE WITH TSPT STATES

Next, we discuss HOM interference with the TSPT states with an arbitrary time delay Δt obtained via temporal post-selection. Figure 3(a) shows the schematic for the time-delayed coincidence measurement between D1 and D2 at the dual output ports of the BS. A photon is measured at D2, and subsequently another photon is measured at D1 after Δt. As can be observed from the Feynman diagrams of Fig. 1(b), the photons in the TSPT state are gathered at the same output port of the PBS, owing to the HOM effect.

Figure 3(b) shows the HOM interferences for $\Delta t = 0$, 40, and 254 ns. The HOM dip fringe with visibility of 50% ± 1% at $\Delta t = 0$ is the nearly same as those observed for $\Delta t = 40$ ns and 254 ns. In the cases of $\Delta t = 40$ ns and 254 ns, the temporal separation between the photons is significantly longer than the 1.01 ps coherence time of the CW coherent photons. The coincidence counting rate of D1 and D2 was measured to be 0.9 kHz with 10 ns and normalized as 0.5 at the path-length difference of 1 mm without the HOM effect. Although the measured photons at D1 and D2 have no temporal correlation with each other, we observe that HOM interference at all Δt values is very similar to that at $\Delta t = 0$. In the study, from the observation of HOM fringes at an arbitrary Δt, we confirmed that HOM interference with temporally separated coherent photons is independent of the time delay Δt. Furthermore, when the electrical delay for the temporal post-selection was replaced with an optical delay with an optical fiber, our results did not change.

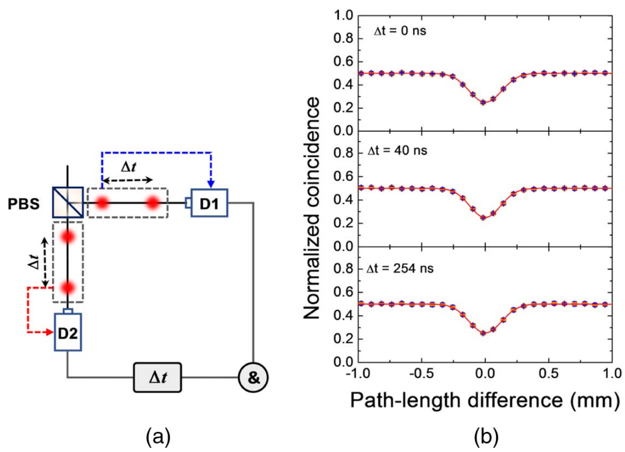

Fig. 3. (a) Schematic for time-delayed coincidence measurement between D1 and D2 at both output ports of the PBS. (b) Normalized coincidence in different spatial modes in the three cases of $\Delta t = 0$, 40, and 254 ns.

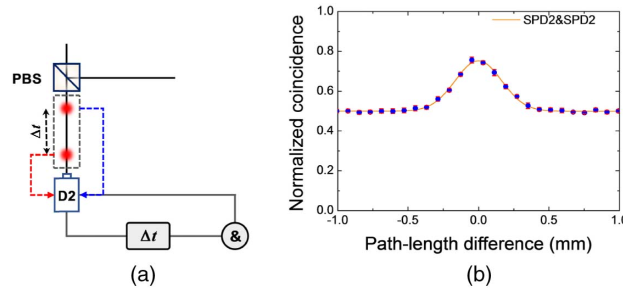

Fig. 4. (a) Schematic for time-delayed coincidence measurement of two photons in identical spatial modes upon performing two consecutive measurements with one SPD (D2). (b) Normalized coincidence in the same spatial modes in the case of $\Delta t = 60$ ns.

To further confirm the HOM effect with TSPT states, we consider time-delayed coincidence measurement in the same spatial mode of the BS by using two consecutive measurements only with D2 as shown in Fig. 4(a) [17]. One photon is measured at D2, and subsequently another photon in the same spatial mode is sequentially measured at D2 after Δt. If the HOM effect occurs with two temporally separated photons in a TSPT state, the first measured photon should be spatially correlated with the time-delayed photon. Therefore, the result of the time-delayed coincidence measurement between the two photons of the TSPT state in the same spatial mode should transpire to be an HOM peak fringe.

Figure 4(b) shows the HOM fringe measured in the same spatial mode with a single SPD under the conditions of $\Delta t = 60$ ns. In particular, the observed HOM peak fringe (obtained via sequential measurements at the single SPD) is remarkable evidence of the HOM effect of temporally separated and uncorrelated photons. The visibility of the HOM peak fringe in Fig. 4(b) is the same as that of the HOM dip fringe in Fig. 3(b). Further, the HOM peak fringe is independent of time delay Δt over a longer time interval than the dead time of the SPD. Therefore, our experimental results become important for extending the HOM effect to photons of TSPT states.

5. HOM INTERFERENCE WITH COHERENT PHOTONS TEMPORALLY SEPARATED BY A DAY

In particular, we next focus on the measurement method for the HOM fringe using photons temporally separated by the order of a day. Here we note that the electrical or optical delay for the temporal post-selection was limited by the constraints of the delay module or the optical fiber loss. To overcome the time-delay limitation, both SPDs were connected to a time-tagging module, and the time-tagged data sets for HOM interference as a function of the path-length difference Δx were obtained by moving the mirror (M2) with a motorized translation stage (Fig. 2). Under the same experimental conditions as before, we measured one set of time-tagged data and independently obtained another set after one day. Here we note that it is possible to measure and store the time-tagged data sets at any time.

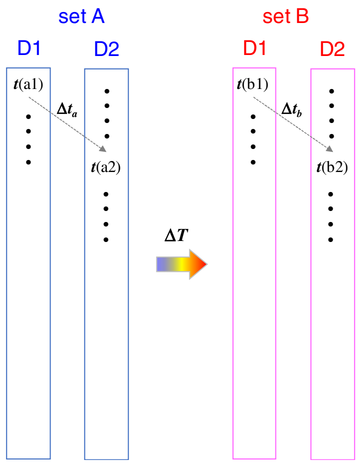

Fig. 5. Analysis method for HOM fringe using photons temporally separated by the order of a day: one set (set A) of time-tagged data and another set (set B) are independently obtained after a long time delay ΔT, where D1 and D2 represent the time data of the detection events at D1 and D2, respectively, corresponding to the two spatial modes of the interferometer arms.

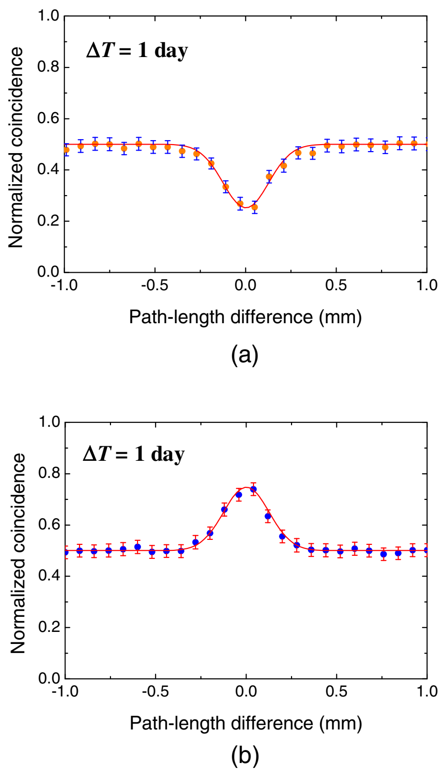

Fig. 6. HOM interference fringe of the TSPT state for $\Delta T = 1$ day. (a) HOM dip fringe (orange circles) of one-day-delayed coincidence counts between D1 data of set A and D2 data of set B; the red curve indicates the fitting of the HOM fringe with visibility of 50% ± 3%. (b) HOM peak fringe (blue circles) of one-day-delayed coincidence counts between D2 data of set A and D2 data of set B in the same spatial modes; the red curve indicates the fitting of the HOM peak fringe.

Let us assume two time-tagged data sets (sets A and B) obtained with both SPDs (D1 and D2) as shown in Fig. 5. Here $t(a1)$ and $t(a2)$ denote the first time-tagged data set of D1 and the time-tagged data set of D2 after time delay Δt_a, respectively, in set A. After a long time delay ΔT, set B is measured under the same conditions as those of set A. In addition, in set B, $t(b1)$ and $t(b2)$ denote the first time-tagged data set of D1 and the subsequent time-tagged data set of D2 after time delay Δt_b, respectively. To obtain the HOM dip fringe of the photons temporally separated by the order of a day, we can analyze arbitrary time-delayed coincidence counts between the D1 data of set A and the D2 data of set B. Furthermore, the HOM peak fringe can be observed via analyzing the day-delayed coincidence counts between the D2 data of set A and the D2 data of set B.

Figure 6 shows the HOM interferences in the case of $\Delta T = 1$ day. In comparison with the results in Figs. 3 and 4, we note that the HOM dip of Fig. 6(a) and HOM peak of Fig. 6(b) of the TSPT state with $\Delta T = 1$ day are nearly identical to the corresponding ones of each data set at $\Delta t = 0$. The coincident count rate was measured to be 0.9 kHz with a 10 ns coincidence window. In our experiment, although the exact value of ΔT is not important, as ΔT increases, the visibility of the HOM fringe is affected because of changes in the experimental environment, such as the alignment of the polarization-based Michelson interferometer and weak coherent light conditions. From the observation of the HOM fringe at the daily time delay ΔT, we can again confirm that HOM interference with temporally separated coherent photons is independent of the time delay.

6. CONCLUSION

In conclusion, we experimentally demonstrated the HOM effect with CW-mode coherent photons temporally well separated by one day via the novel post-selection method using time-tagged data sets. We obtained the HOM dip and peak fringes with 0.5 limited maximum visibility of the temporally separated coherent photons via the utilization of two different setups for arbitrary time-delayed coincidence measurement in the cases of different spatial modes with two SPDs and the same spatial modes with a single SPD. From these results, we confirmed that the two temporally separated photons in a TSPT state are probabilistically gathered at one of the two PBS output ports regardless of the large temporal separation between the photons. This intriguing HOM effect can be understood as the indistinguishability of the two-photon probability amplitudes of the two photons in the TSPT states. We believe that our results can contribute to a greater understanding of two-photon quantum interference from the perspective of quantum physics and aid in elucidating the HOM interference effect, which is essentially utilized in many quantum information protocols including quantum communication and optical quantum-information processing.

Funding. National Research Foundation of Korea (2018R1A2A1A19019181).

Disclosures. The authors declare no conflicts of interest.

REFERENCES

1. P. A. M. Dirac, *The Principles of Quantum Mechanics*, 4th ed. (Oxford University, 1958).
2. C. K. Hong, Z. Y. Ou, and L. Mandel, “Measurement of subpicosecond time intervals between two photons by interference,” Phys. Rev. Lett. **59**, 2044–2046 (1987).
3. P. Hariharan and B. C. Sanders, “Quantum phenomena in optical interferometry,” in *Progress in Optics*, E. Wolf, ed. (Elsevier, 1996), pp. 49–128.
4. G. Jaeger and A. V. Sergienko, “Multi-photon quantum interferometry,” in *Progress in Optics*, E. Wolf, ed. (Elsevier, 2001), pp. 277–324.
5. J. W. Pan, Z. B. Chen, C. Y. Lu, H. Weinfurter, A. Zeilinger, and M. Żukowski, “Multiphoton entanglement and interferometry,” Rev. Mod. Phys. **84**, 777–838 (2012).
6. E. Knill, R. Laflamme, and G. J. Milburn, “A scheme for efficient quantum computation with linear optics,” Nature **409**, 46–52 (2001).
7. P. Kok, W. J. Munro, K. Nemoto, T. C. Ralph, J. P. Dowiling, and G. J. Milburn, “Linear optical quantum computing with photonic qubits,” Rev. Mod. Phys. **79**, 135–174 (2007).
8. L. Mandel, “Quantum effects in one-photon and two-photon interference,” Rev. Mod. Phys. **71**, S274–S282 (1999).
9. T. Jung, Y.-S. Lee, J. Park, H. Kim, and H. S. Moon, “Quantum interference between autonomous single-photon sources from Doppler-broadened atomic ensemble,” Optica **4**, 1167–1170 (2017).
10. J. Park, H. Kim, and H. S. Moon, “Two-photon interferences of non-degenerate photon pairs from Doppler-broadened atomic ensemble,” Opt. Express **25**, 32064–32073 (2017).
11. J. Fulconis, O. Alibart, J. L. O’Brien, W. J. Wadsworth, and J. G. Rarity, “Nonclassical interference and entanglement generation using a photonic crystal fiber pair photon source,” Phys. Rev. Lett. **99**, 120501 (2007).
12. S. Rogers, D. Mulkey, X. Lu, W. C. Jiang, and Q. Lin, “High visibility time-energy entangled photons from a silicon nanophotonic chip,” ACS Photon. **3**, 1754–1761 (2016).
13. Z. Y. Ou, E. C. Gage, B. E. Magill, and L. Mandel, “Fourth-order interference technique for determining the coherence time of a light beam,” J. Opt. Soc. Am. B **6**, 100–103 (1989).
14. Y. Miyamoto, T. Kuga, M. Baba, and M. Matsuoka, “Measurement of ultrafast optical pulses with two-photon interference,” Opt. Lett. **18**, 900–902 (1993).
15. Y.-S. Kim, O. Slattery, P. S. Kuo, and X. Tang, “Conditions for two-photon interference with coherent pulses,” Phys. Rev. A **87**, 063843 (2013).
16. Y.-S. Kim, O. Slattery, P. S. Kuo, and X. Tang, “Two-photon interference with continuous-wave multi-mode coherent light,” Opt. Express **22**, 3611–3620 (2014).
17. H. Kim, S. M. Lee, O. Kwon, and H. S. Moon, “Observation of two-photon interference effect with a single non-photon-number resolving detector,” Opt. Lett. **42**, 2443–2446 (2017).
18. K. Wang and D.-Z. Cao, “Subwavelength coincidence interference with classical thermal light,” Phys. Rev. A **70**, 041801(R) (2004).
19. P. Hong, J. Liu, and G. Zhang, “Two-photon superbunching of thermal light via multiple two-photon path interference,” Phys. Rev. A **86**, 013807 (2012).
20. J. Xiong, D.-Z. Cao, F. Huang, H.-G. Li, X.-J. Sun, and K. Wang, “Experimental observation of classical subwavelength interference with a pseudo thermal light source,” Phys. Rev. Lett. **94**, 173601 (2005).
21. J. Liu, H. Zheng, H. Chen, Y. Zhou, F.-L. Li, and Z. Xu, “The first- and second-order temporal interference between thermal and laser light,” Opt. Express **23**, 11868–11878 (2015).
22. T. B. Pittman, D. V. Strekalov, A. Migdall, M. H. Rubin, A. V. Sergienko, and Y. H. Shih, “Can two-photon interference be considered the interference of two photons?” Phys. Rev. Lett. **77**, 1917 (1996).
23. Y.-H. Kim, M. V. Chekhova, S. P. Kulik, and Y. Shih, “Quantum interference by two temporally distinguishable pulses,” Phys. Rev. A **60**, R37 (1999).
24. Y.-H. Kim, “Two-photon interference without bunching two photons,” Phys. Lett. A **315**, 352 (2003).
25. Y.-H. Kim and W. P. Grice, “Quantum interference with distinguishable photons through indistinguishable pathways,” J. Opt. Soc. B **22**, 493 (2005).
26. H. Kim, S. M. Lee, and H. S. Moon, “Two-photon interference of temporally separated photons,” Sci. Rep. **6**, 34805 (2016).